Electronic Supplementary Information

Characterization

The crystalline structure of the sample was characterized by using X-ray diffractometer (Bruker AXS D8 Advance). The compositions and micro-structures of the samples was further analyzed by field emission scanning electron microscopy (FESEM, Hitachi S-4800) and transmission electron microscopy (TEM, FEI Talos F200x) equipped with an energy dispersive X-ray spectrometer (EDS). X-ray photoelectron spectroscopy (XPS) measurements were performed using a Thermo Scientific K-Alpha spectrometer. Fourier transform infrared (FTIR) spectra were measured using a NICOLET-5700 FTIR spectrophotometer.

Electrochemical measurements

Galvanostatic charge-discharge (GCD), cyclic voltammetry (CV) and electrochemical impedance spectroscopy (EIS) measurements were measured on a CHI660E electrochemical workstation (Shanghai chenhua). All experiments were performed at ambient temperature.

Three-electrode experiments were performed in an aqueous solution containing 2 M KOH. NiCoS/CeO_2/NF ($1\times1 cm^2$), a saturated calomel electrode (SCE) and a platinum foil electrode were used as working electrodes, reference electrode and counter electrode, respectively.

For the two-electrode test, the ASC was constructed with a working

electrode ($NiCoS/CeO_2/NF$) and an activated carbon (AC) electrode. Activated carbon electrodes were made by mixing the active material, conductive agent (acetylene black), and polyvinylidene fluoride (PVDF) in a mass ratio of 8:1:1, then adding a few drops of 1-methyl-2-pyrrolidone (NMP) to form a slurry, which was coated on the surface of a foamed nickel substrate (1×3 cm^2), dried and pressed finally.

The specific capacitance (C_s, F/g) of the electrode materials is calculated as follows:

$$C_s = \frac{I \times \Delta t}{m \times \Delta V} \quad (S1)$$

where I (A), ΔV (V), Δt (s) and m (g) represent the current, voltage window, discharge time and mass of active materials, respectively.

To assemble the ASC device, the amounts of charge (Q) carried by the anode and cathode should be balanced by the following equation:

$$Q_- = m_- \times C_- \times \Delta V_- = m_+ \times C_+ \times \Delta V_+ = Q_+ \quad (S2)$$

where C (F/g), ΔV (V) and m (g) are the specific capacitance, potential window and mass of active materials, respectively.

The energy density (E, Wh/kg) and power density (P, W/kg) of the $V_2O_5@Co_3S_4$-5h//AC cell is calculated as follows:

$$E = \frac{C_s \times (\Delta V)^2}{2 \times 3.6} \quad (S3)$$

$$P = \frac{3600 \times E}{\Delta t} \quad (S4)$$

where C_s (F/g), ΔV (V) and t (s) are the specific capacitance, voltage window and

discharging time, respectively.

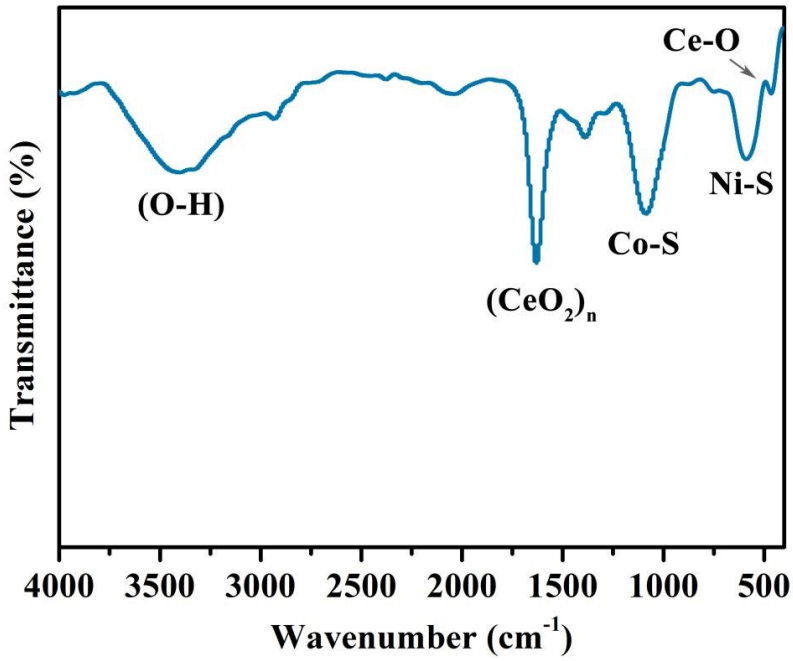

Fig. S1. FTIR spectrum of $NiCoS/CeO_2$.

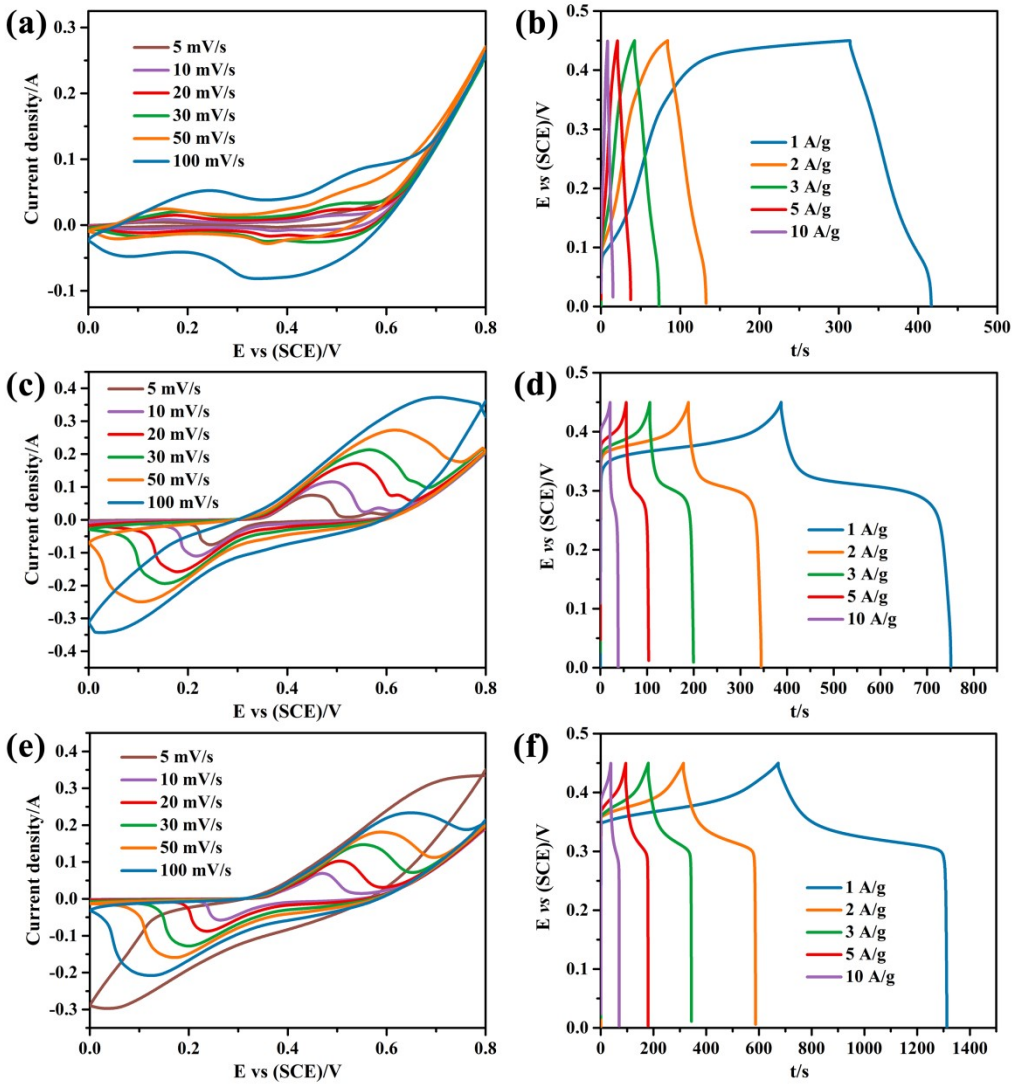

Fig. S2. (a, c, e) CV and (b, d, f) GCD curves of the (a, b) ZIF-L, (c, d) NiCo-LDH and (e, f) NiCoS.

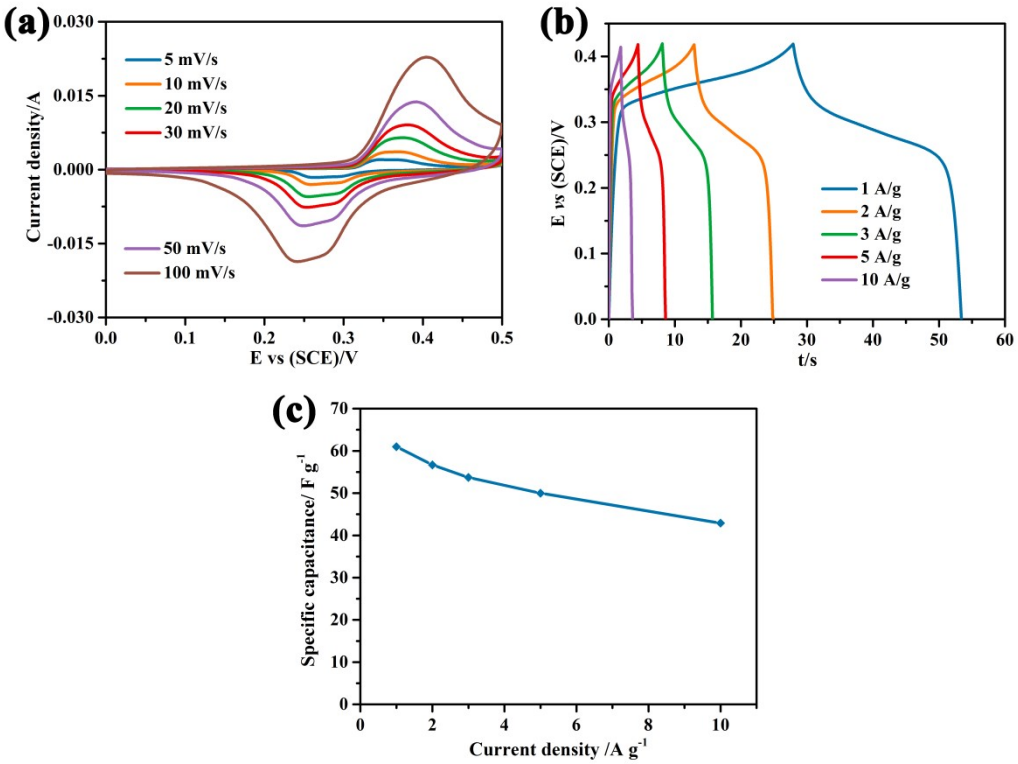

Fig. S3. (a) CV curves, (b) GCD curves and (c) specific capacitances of the CeO_2.

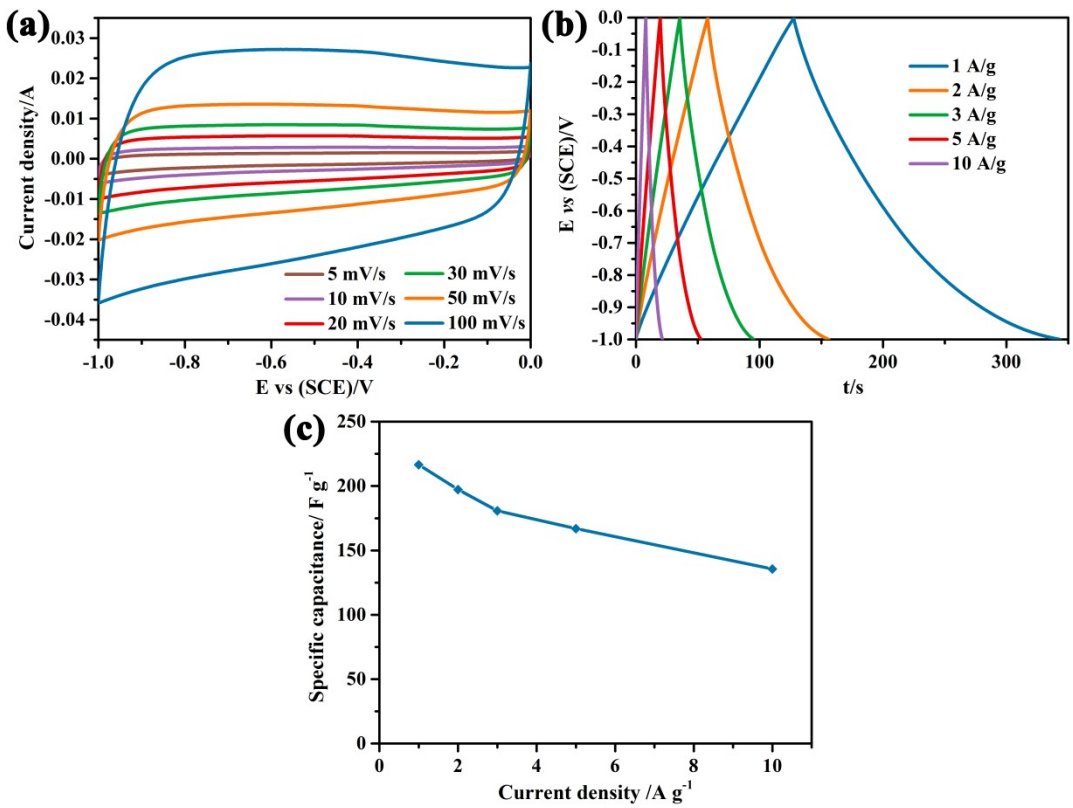

Fig. S4. (a) CV curves, (b) GCD curves and (c) specific capacitances of the AC electrode.

Table S1. Comparison of $NiCoS/CeO_2$ with previously reported electrode materials

electrode materials	current density	specific capacitance	reference
$NiCoS/CeO_2$	1 A g^{-1} 10 A g^{-1}	2840.2 F g^{-1} (1278.1 C g^{-1}) 1582.3 F g^{-1} (712 C g^{-1})	**this work**
CeO_2@$(Ni, Co)_3S_4$	1 A g^{-1}	1319 F g^{-1}	1
Co_3S_4/CeO_2-NPAs	1 A g^{-1}	2310 F g^{-1} (1108.8 C g^{-1})	2
NiCoS@PPy	1 A g^{-1}	2316.7 F g^{-1}	3
ZnO/CoO@NiCoS nanoarrays	1 A g^{-1}	934 C g^{-1}	4
CeO_2/Ni-Al LDH	1 A g^{-1}	879.6 F g^{-1}	5
PANI/CeO_2/$Ni(OH)_2$	1 A g^{-1}	2556 F g^{-1}	6
$NiCo_2O_4/CeO_2$	10 A g^{-1}	1312.3 F g^{-1}	7
rGO-Ni-Mo-oxide@Ni-Co-S core-shell nanotubes	1 A g^{-1}	2867 F g^{-1}	8
CeO_2@NiFeLDH	1 A g^{-1}	516.5 F g^{-1}	9
NiCoS/d-Ti_3C_2	1 A g^{-1}	758.9 C g^{-1}	10
$CoMoS_4$@Ni-Co-S nanotubes	1 A g^{-1}	2208.5 F g^{-1}	11

Table S2. EIS fitting results of the samples

	ZIF-L	NiCo-LDH	NiCoS	NiCoS /CeO_2
R_s (Ω)	0.8546	0.8223	0.6824	0.6228
R_{ct} (Ω)	0.5196	0.4167	0.4976	0.3338

References

1. Z. Xue, C. Yang, K. Tao and L. Han, Heterostructure of metal–organic framework-derived straw-bundle-like CeO_2 decorated with (Ni, $Co)_3S_4$ nanosheets for high-performance supercapacitor, *Applied Surface Science*, 2022, **592**, 153231.
2. Z. Xue, L. Lv, Y. Tian, S. Tan, Q. Ma, K. Tao and L. Han, Co_3S_4 Nanoplate Arrays Decorated with Oxygen-Deficient CeO_2 Nanoparticles for Supercapacitor Applications, *ACS Applied Nano Materials*, 2021, **4**, 3033-3043.
3. X. Zhao, Q. Ma, K. Tao and L. Han, ZIF-Derived Porous $CoNi_2S_4$ on Intercrosslinked Polypyrrole Tubes for High-Performance Asymmetric Supercapacitors, *ACS Applied Energy Materials*, 2021, **4**, 4199-4207.
4. Y. He, X. Zhou, S. Ding, Q. Hu, D. Lin and X. Wei, ZnO/CoO@NiCoS nanohybrids with double heterogeneous interface for high-performance hybrid supercapacitors, *Journal of Alloys and Compounds*, 2021, **875**, 160046.
5. J. Zheng, J. Wang, J. Qu, M. Wu and Z. Xu, CeO_2/Ni-Al layered double hydroxide composite electrode for the enhancement of specific capacitance and capacitance retention performance, *Applied Clay Science*, 2022, **216**, 106370.
6. Q. Guo, J. Yuan, Y. Tang, C. Song and D. Wang, Self-assembled PANI/CeO_2/$Ni(OH)_2$ hierarchical hybrid spheres with improved energy storage capacity for high-performance supercapacitors, *Electrochimica Acta*, 2021, **367**, 137525.
7. G. Santhosh, G. P. Nayaka and A. S. Bhatt, Ultrahigh capacitance of $NiCo_2O_4$/CeO_2 mixed metal oxide material for supercapacitor applications, *Journal of Alloys and Compounds*, 2022, **899**, 163312.
8. J. Acharya, G. P. Ojha, B. S. Kim, B. Pant and M. Park, Modish Designation of Hollow-Tubular rGO-NiMoO4@Ni-Co-S Hybrid Core-shell Electrodes with Multichannel Superconductive Pathways for High-Performance Asymmetric Supercapacitors, *ACS Appl Mater Interfaces*, 2021, **13**, 17487-17500.
9. T. Zhou, W. Zhang, H. Fu, J. Fang, C. Chen and Z. Wang, Preparation of 3D CeO_2@NiFe-LDH composites derived from prussian blue analogues for high performance supercapacitors, *Materials Science in Semiconductor Processing*, 2022, **150**, 106913.
10. Y. Luo, Y. Tian, Y. Tang, X. Yin and W. Que, 2D hierarchical nickel cobalt sulfides coupled with ultrathin titanium carbide (MXene) nanosheets for hybrid supercapacitors, *Journal of Power Sources*, 2021, **482**, 228961.
11. F. Ma, X. Dai, J. Jin, N. Tie and Y. Dai, Hierarchical core-shell hollow $CoMoS_4$@Ni–Co–S nanotubes hybrid arrays as advanced electrode material for supercapacitors, *Electrochimica Acta*, 2020, **331**, 135459.